# Physical - Empirical Model for Generation of Multi Component Synthetic Ground Motion Time Histories at Closely Spaced Distances


**M.I. Todorovska, M.D. Trifunac & V.W. Lee**
*Univ. of Southern California, Dept. of Civil Eng., Los Angeles, CA, 91089-2431, U.S.A.*

**N. Orbović**
*Canadian Nuclear Safety Commission, Ottawa, Ontario K1P 5S9, Canada*

**SUMMARY:**
Linear and especially nonlinear analyses of spatially extended structures, such as pipelines and bridges, often requires time histories of ground motion at an array of closely spaced points. As the number of such earthquake observations is small worldwide, synthetic motions with desired characteristics become necessary. A method for synthesizing such site specific motions is presented, which is an extension of the SYNACC method, developed earlier for a point. It consists of unfolding in time a site specific Fourier amplitude spectrum of ground acceleration, obtained by an empirical scaling model, by representing the ground motion as a superposition of travelling wavelets of Love and Rayleigh waves and body waves, which propagate with phase and group velocities consistent with the site geology, approximated by parallel layers. The method generates synthetic accelerations, velocities, displacements, near surface strains, rotations and curvatures of ground motion. The method is illustrated for scenario M6.5 and M7.5 earthquakes.

*Keywords: synthetic ground motion; artificial accelerograms; ground strains; ground rotations; SYNACC.*

## 1. INTRODUCTION

The method presented is an extension of the SYNACC method, first proposed by Trifunac (1971), which evolved over the years, by inclusion of more current empirical scaling laws for Fourier amplitude spectra of acceleration and frequency dependent duration Wong and Trifunac (1978,1979), and extension to prediction of rotational motions (Lee and Trifunac, 1985a, 1987), strains (Lee 1990) and curvature (Trifunac, 1990), all at a point in space (see also review in Lee (2002)). This paper presents an extension to generating related motions at an array of points on the ground surface. Another difference is the introduction of "distance from the edge of the valley", which is smaller than the distance from the source, and which helps control the duration of the record. Further, the expressions for the point strains, rotations and curvatures, derived from the new formulation, differ slightly from the previous ones, which do not include spatial derivatives of the amplitude modulation of the travelling wavelets. A more detailed presentation of the method and additional examples can be found in Todorovska et al. (2012). In what follows, for brevity, we will use "pipeline" to mean any long structure supported by many separate foundations.

The method is based on representation of the ground motion by traveling wavelets of surface and body waves, which propagate in space with phase and group velocities that are those of a horizontally layered half-space approximating the soil and geology of the site. The amplitudes of the wavelets are such that the total motion in a narrow frequency band matches a target Fourier amplitude spectrum of acceleration. The methodology has been implemented in a computer program, which has built in a suite of empirical scaling models for prediction of site specific Fourier amplitude spectra of acceleration, and computes the phase and group velocities specific for the site. A uniform hazard spectrum, or any user specified spectrum can also be used. While the Fourier spectrum determines the overall amplitudes of motion, the layered structure determines the distribution of the energy in time at a given site, and also the causal relationship between the motions at neighboring points along the

supports of the structure. This causal relationship is such that the motions further away from the source are delayed relative to the closer points differently in different frequency bands. Examples are shown of time histories for ground accelerations, velocities and displacements in the radial, transverse and vertical direction, and radial (normal) and transverse (shear) strains, at a point and at an array of points.

This physical model – empirical method has clear advantages over both the engineering stochastic methods and the seismological physics based methods. The former methods (see recent comprehensive review in Zerva (2009)) produce motions with stationary frequency content over the entire duration, in contrast to the nonstataionary nature reveled by the many observations. Further, motions at an array of points are generated using overly simplified coherency function, which is based on a single valued phase velocity, rather than the complete site-specific set for all body waves and surface wave modes. The latter methods involve numerical simulations based on a physical model of the earthquake source and of the wave propagation from the source to the site. They produce motions with correct physical nature, but involve many assumptions and need to be validated with data. Also, due to the lack of detail in the available information about the earthquake source and the wave path, they have difficulties to model high-frequency content of the synthetic motions. The SYNACC method, which is neither stochastic nor purely physics based, does not suffer from these shortcomings. It produces motions with amplitudes that are, by definition, consistent with observations over a broad frequency range. Also, the motions are nonstationary in a physically meaningful sense and consistent with the site soil and geology.

## 2. METHODOLOGY

The geology between the earthquake source and the site can vary considerably, especially for large distances, and different types of waves will arrive at the site via different wave paths, as illustrated in Fig. 1, showing the earthquake fault, and a segment of a pipeline located on sediments. The surface waves (Love and Rayleigh) arrive horizontally through the low velocity layers, with velocities that are

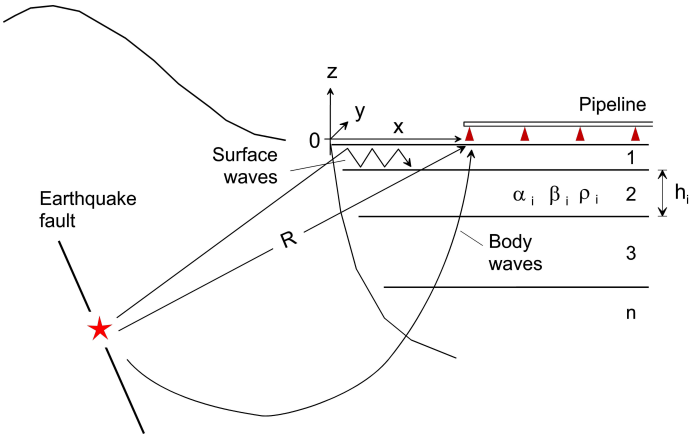


**Fig. 1** Model.

frequency dependent, defined by the dispersion in the layers of site soil and geology, while the body waves arrive from depth at an angle, which is close to vertical for soft geology near the surface. Further, the amplitude attenuation is different for body and surface waves, due to different geometric spreading, and for both waves, the attenuation is frequency dependent. The *total* effect can be predicted reliably, in statistical sense, using empirical scaling laws for Fourier amplitude spectra of acceleration. Considering the nature of these processes, in the SYNACC methodology, over the frequency band of interest, 0 to 25 Hz, the empirically predicted Fourier amplitude spectrum is partitioned in $N$ narrow non-overlapping subbands, and the energy in each subband is partitioned

among surface and body waves. Waves in a narrow frequency band propagate as groups, forming wavelet packets, the amplitudes of which are localized in time, and propagate with their group velocity. The total motion, therefore, can be represented as a superposition of such wavelet packets. In the following, the representation of the surface and body waves that enables generation of related motions at an array of points is presented.

### 2.1 Representation of Surface Wave Motion at a Site

To expand the surface waves, the soil and geology at the site is locally approximated by a horizontally layered half-space, as shown in Fig. 1. Let $h_i$, $\rho_i$, $\alpha_i$ and $\beta_i$ be the thickness, mass density and P- and S-wave velocities in the $i$-th layer, with $i = 1, \ldots, L$, and let the $x$-axis point in the direction of wave propagation. The layer boundaries define a boundary value problem for the displacement, which has a solution that is a surface wave only for a discrete set of frequency dependent phase velocities $c_m(\omega)$, obtained from the roots of the characteristic equation for the particular problem (Thompson 1950; Haskell 1953; Mahta et al. 2007). The displacement for an eigenvalue constitutes an eigenfunction (or a mode), and any surface wave motion then can be represented as a linear combination of these eigenfunctions.
Fig. 2 shows an example of a velocity profile, proposed by Trifunac (1971) to approximate the

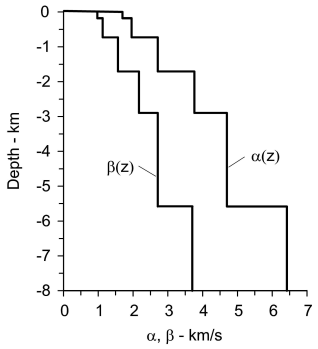


**Fig. 2** Site velocity profile.

**Table 1** Profile for dispersion model 3

| No. | $h$ [km] | $\alpha$ [km/s] | $\beta$ [km/s] | $\rho$ [gm/cm$^3$] |
|---|---|---|---|---|
| 1a | 0 .03 | 0.4335 | 0.25 | 1.20 |
| 1b | 0.03 | 0.867 | 0.50 | 1.2 |
| 1c | 0.12 | 1.70 | 0.98 | 1.28 |
| 2 | 0.55 | 1.96 | 1.13 | 1.36 |
| 3 | 0.98 | 2.71 | 1.57 | 1.59 |
| 4 | 1.19 | 3.76 | 2.17 | 1.91 |
| 5 | 2.68 | 4.69 | 2.71 | 2.19 |
| 6 | $\infty$ | 6.40 | 3.70 | 2.71 |

geology of a site in El Centro in Imperial Valley, California, and used in subsequent work. In Todorovska et al. (2012), we show examples for this profile and also for two of its variants, which are softer in the top 180 m. In this paper, we show only results for the variant referred to as dispersion model 3. Table 1 shows the properties of the layers for that model we use in this paper, and Fig. 3 shows the phase and group velocities, $c_m(\omega)$ and $U_m(\omega)$ $m = 1, \ldots, 5$, for the first five modes of Rayleigh and Love waves, for all the three variants. The Rayleigh waves are surface waves with in-plane particle motion along an ellipse, which is usually retrograde at the surface, and with vertical to horizontal aspect ratio > 1. The Love waves are surface waves with out of plane particle motion. The group velocity $U_m(\omega) \triangleq d\omega / dk_m$, where $k_m(\omega) \triangleq \omega / c_m(\omega)$ is the horizontal wave number, is the velocity with which the amplitude envelope of the wavelet packet propagates, and with which the energy is transported. The number of modes is finite for a given frequency, and increases with frequency. The first mode exists at all frequencies, while the higher modes exist only for high enough frequencies. The phase and group velocities for high frequencies approach asymptotically the shear wave velocity of the top layer for the model, which is the softest.

The synthesis is based on dividing the frequency band of interest, 0 to 25 Hz, in $N$ non-overlapping subbands, assuming uniform Fourier amplitude within the subband, and in each band, representing the surface wave motion as a superposition of the eigenfunctions, evaluated at the central frequency of the subband. Let $\omega_n$ and $\Delta\omega_n$ be the central frequency and half-bandwidth of the $n$-the subband, $U_{nm} = U_m(\omega_n)$ and $c_{nm} = c_m(\omega_n)$ be the group and phase velocities of the $m$-th mode in that

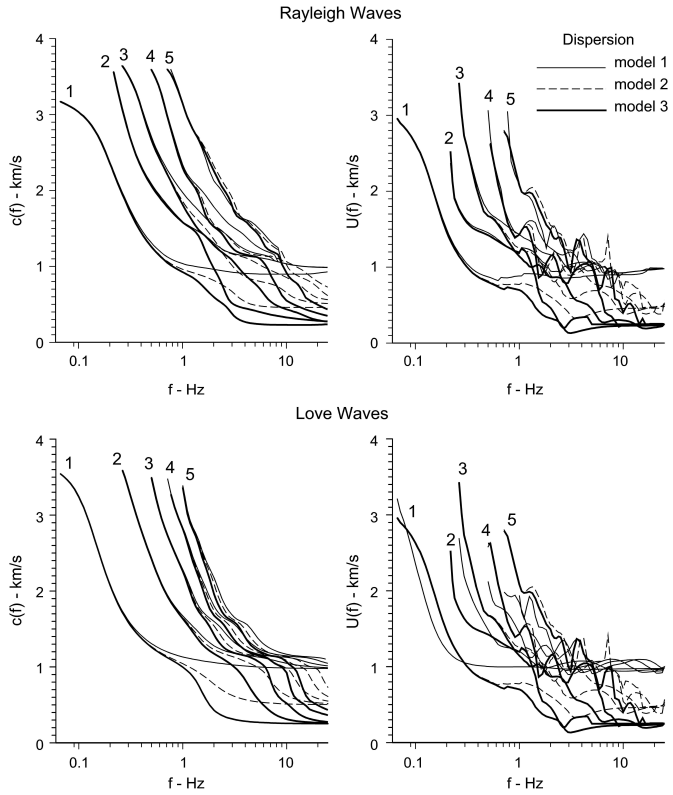


**Fig. 3** Phase velocities $c(f)$ (left) and group velocities $U(f)$ (right) for Rayleigh and Love waves, for three geology profiles, differing only in the top 180 m.

subband, and let $w_{nm}(x;t)$ be the eigenfunction of the $m$-th mode in the $n$-th subband, at point $x$ on the free surface ( $z = 0$ ), and at time $t$. Then

$$w_{nm}(x;t) = \mathrm{sinc}\left[\Delta\omega_n\left(t - \frac{x}{U_{nm}}\right)\right]\exp\left[i\left(\omega_n t - k_{nm}x\right)\right] \tag{1}$$

where

$$k_{nm} = \frac{\omega_n}{c_{nm}}\left(1 - i\frac{1}{2Q}\right) \tag{2}$$

is the complex horizontal wave number, and $Q$ is the quality factor, assumed to be constant (Trifunac, 1994). If no material attenuation is assumed, $1/(2Q) = 0$ and $k_{nm}$ is real. Function $w_{nm}(x;t)$ represents a traveling wavelet, which is a complex exponential of frequency $\omega_n$, amplitude modulated by a sinc function. The amplitude modulation

$$\mathrm{sinc}\left(\Delta\omega_n t\right) = \frac{\sin(\Delta\omega_n t)}{\Delta\omega_n t} \tag{3}$$

is a window in time with half-width $\Delta t_n = \pi/\Delta\omega_n$, which propagates with velocity $U_{nm}$, while the phase propagates with velocity $c_{nm}$. Consequently, at a point $x$, the phase has time lag $x/c_{nm}$, and the center of the amplitude envelope has time lag $x/U_{nm}$ relative to the reference point, $x = 0$.

Then, the Fourier transform of the wavelet $w_{nm}(x;t)$ is

$$\hat{w}_{nm}(x;\omega) = \frac{\pi}{\Delta\omega_n}\exp\left[-i\left(\frac{\omega-\omega_n}{U_{nm}}+k_{nm}\right)x\right]p_{\Delta\omega_n}(\omega-\omega_n) \tag{4}$$

where

$$p_{\Delta\omega_n}(\omega-\omega_n) = \begin{cases} 1, & \omega-\Delta\omega_n \le \omega \le \omega_n+\Delta\omega_n \\ 0, & \text{otherwise} \end{cases} \tag{5}$$

represents a box function with half width $\Delta\omega_n$, centered at frequency $\omega_n$, with amplitude scaled to $\pi/\Delta\omega_n$ and phase shifted by $k_{nm}x$.

According to Eqns (1) and (4), the energy of the wavelet $w_{nm}(x)$ is localized, in time - around $t = x/U_{nm}$ with spread $\pm\Delta t_n = \pm\pi/\Delta\omega_n$, and, in frequency, around $\omega = \omega_n$ with spread $\pm\Delta\omega_n$, i.e. within a rectangle of constant area $(2\Delta t_n)(2\Delta\omega_n) = 2\pi$ in the phase plane. Consequently, finer division of the frequency range (smaller $\Delta\omega_n$) will lead to wider in time wavelets $w_{nm}(x;t)$, which is a manifestation of the Heisenberg-Gabor uncertainty principle for signals (Gabor 1946, 1953).

Let $u(x,t)$ be the associated analytic signal of a generic component of motion (the specific expansions will be presented in one of the following sections. Because scaling laws for Fourier spectra of acceleration are available, we start with the representation of acceleration in a series of wavelets

$$\ddot{u}(x,t) = \sum_{n=1}^{N}\sum_{m=1}^{M_n} A_{nm}^{*} w_{nm}(x;t) \tag{6}$$

where $M_n$ is the number of modes that exist in the $n$-th subband.

The coefficients of the expansion $A_{nm}^{*}$ are complex valued and depend on the amplitude of the target spectrum, but, for a given site geology, they are related, as shown in (Trifunac 1971) for a site in Imperial Valley, and their relative amplitude depends on the frequency and mode number. We represent them as

$$A_{nm}^{*} = \alpha_n A_1(m) A_2(\omega_n)\exp\left(i\phi_{nm}^{ran}\right) \tag{7}$$

where $\phi_{nm}^{ran}$ is a random phase between $-\pi$ and $\pi$, describing the randomness in the radiation of energy from the earthquake source and other randomness along the wave path until the arrival to the region near the site, represented by the medium with parallel layers (Fig. 1). Functions $A_1(m)$ and $A_2(\omega_n)$ are site specific, and their product $A_1(m)A_2(\omega_n)$ can be thought of as a site dependent mode participation factor. The coefficients $\alpha_n = \alpha(\omega_n, \Delta\omega_n)$, for given division in subbands, depends only on the target spectrum that is to be matched by the synthetics.

The representation (6) differs from the previous representation as follows. In the latter, the phase delay at point $x$ is $(\omega_n/U_{mn})t + \phi_{nm}^{ran}$, i.e. the lag of the amplitude modulation plus some random phase shift, while in this paper, the phase lag is $(\omega_n/c_{mn})t$. In this paper, we consider also material attenuation due to $Q$, which affects the difference between the motion at different points of the array. A minor difference is that the random phase is part of the coefficients of expansion, and that the associated analytic signal is expanded. Another significant difference is in the definition of the

reference point $x = 0$. In the latter, $x = 0$ is the epicenter of the earthquake, while, in this work, it is a point between the epicenter and the site, from where the parallel layers geology can be adopted to be representative of the wave path. This point can be referred to as the "the edge of the valley", and $x =$ representative distance from the edge of the valley. Therefore, in this paper, $x$ is just the distance over which dispersive wave propagation occurs consistent with the given parallel layers of soil and geology, while the target spectrum to be matched depends on the hypocentral distance $R$ of the site from the source (Fig. 1). Such definition of the reference $x = 0$ is more useful for modeling, as the geology can vary considerably between the source and the site. It also helps control the duration of the synthetic motion, and avoid the artifact of unrealistically long duration of the synthetic motion for large source to site distances and softer near surface soil layers. Because the parallel layers structure is an idealization, the "distance from the edge of the valley" is not exact but an abstraction, and can be chosen by trial and error or by iteration, until the duration of the synthetic motion is satisfactory, based on some subjective or objective standard, such as empirical scaling laws.

### 2.2 Expansion of Body Waves

The propagation of body waves is essentially nondispersive, and $c(\omega_n) = U(\omega_n)$. They arrive at the site from depth, often close to vertical due to progressive bending of the rays towards the surface (Fig. 1), and consequently propagate horizontally with larger phase velocities $c(\omega_n)$ than the surface waves. Further, their amplitude at a given frequency reflects the interference characteristics of the layers, which depends on incident angle. In the SYNACC synthesis, the body waves are treated as two additional "surface wave modes", one for P- and the other one for S-waves, with large phase/group velocities, and contributing respectively to the in-plane and out of plane motions, and with mode participation factor same as those for the Love modes, i.e. not reflecting the site interference characteristics, but with the flexibility to increase or decrease their participation, relative to that of the surface waves. Site specific interference features could be included by appropriate frequency dependent mode participation factors, derived e.g. using the propagator matrix of the medium (Mehta et al. 2007). Pipelines, however, are light, long and flexible structures, hence more sensitive to strains and differential motions, which are caused largely by the surface waves, and including the site interference (resonances) is not essential.

### 2.3 Expansion Coefficients for a Site and Motion at an Array of Sites

The site specific mode participation factors, $A_1(m)A_2(\omega_n)$, can be determined by analysis of recorded motion in the region, as in Trifunac (1971). In this paper, we use the same functions. The coefficients $\alpha_n$ are determined from the requirement that some representative value of $\left|\hat{\ddot{u}}(x;\omega)\right|$ over the $n$-th subband matches a target value, $FS^{tar}(\omega_n)$. For example, such representative value can be obtained by averaging $\log_{10}\left|\hat{\ddot{u}}(x;\omega)\right|$ and converting back to linear scale.

The sites where related motions are needed for analysis of extended structures are typically at distances from few tens of meters to few kilometers. For such distances, it is assumed that the motion differs only because of deterministic propagation and attenuation due to $Q$, while the randomness in phase and mode participation factors, included in coefficients $A^*_{nm}$, is the same. For such an array of sites, the motion at one representative site, at $x = x_0$, is first synthesized by matching the target spectrum, which gives the coefficients $A^*_{nm}(x_0)$, and the motion at another sites, at $x = x_0 + \Delta x$, is then computed as

$$\hat{\ddot{u}}(x_0 + \Delta x, \omega) = \sum_{n=1}^{N} \sum_{m=1}^{M_n} A^*_{nm}(x_0)\hat{w}_{nm}(x_0 + \Delta x; \omega) \tag{8}$$

### 2.4 Components of Linear Motions, Strains, Rotations and Curvatures

Let $\ddot{u}_x(x;t)$, $\ddot{u}_y(x;t)$ and $\ddot{u}_z(x;t)$ be the components of acceleration along the coordinate axes as in Fig. 1, each having their own expansion. Because $u_x(x;t)$ and $u_z(x;t)$ are expanded in Rayleigh modes, the expansion wavelets $\hat{w}^x_{nm}(x;\omega)$ are as in Eqn. (4) with group and phase velocities $U^R_{nm}$ and $c^R_{nm}$ specific for the mode, and $\hat{w}^z_{nm}(x;\omega) = V_{nm}\hat{w}^x_{nm}(x;\omega)$ where $V_{nm} = V_m(\omega_n)$ is the complex ratio of vertical to horizontal amplitude of the elliptic particle motion at the surface for the mode. Similarly, $u_y(x;t)$ is expanded in Love modes, and $\hat{w}^y_{nm}(x;\omega)$ are as in Eqn. (4) with group and phase velocities $U^L_{nm}$ and $c^L_{nm}$ specific for the mode. The corresponding representations of velocities, displacements, strains, rotations and curvatures can be easily obtained in the frequency domain from the representations of acceleration, and the analytical temporal and spatial derivatives of the wavelets. The point axial and transverse shear strains are obtained from

$$\hat{\varepsilon}_{xx}(x;\omega) = \frac{\partial}{\partial x}\hat{u}_x(x;\omega); \quad \hat{\varepsilon}_{xy}(x;\omega) = \frac{1}{2}\frac{\partial}{\partial x}\hat{u}_y(x;\omega) \tag{9}$$

the vector point rotation is obtained from

$$\vec{\psi}(x;\omega) = \nabla \times \vec{u}(x;\omega) \tag{10}$$

and the curvatures are obtained from the second derivatives of displacement (complete expression are presented in Todorovska et al. (2012).

### 2.5 Generation of Target Spectrum

Site specific target Fourier amplitude spectra for a *scenario* earthquake can be generated using an empirical scaling model for a Fourier amplitude spectrum, for given earthquake magnitude, hypocentral distance, site conditions, and probability of being exceeded, which reflects the uncertainty in the scaling law. The uncertainty in the earthquake size, location and occurrence rate can also be included by specifying as a target spectrum a uniform hazard Fourier spectrum, which has amplitudes with equal probability of being exceeded from any earthquake considered.

Program SYNACC has built in the empirical scaling models from Trifunac and Lee (1985) and Trifunac (1976, 1979, 1989a,b), and can also use uniform hazard spectrum compatible with output of program NEQRISK (Lee and Trifunac 1985b), which has built in the same scaling models, or any user provided Fourier amplitude spectrum. The built in scaling models differ in the input parameters, and a particular model can be chosen depending on how detailed information in available for the site. For example, earthquake magnitude or Modified Mercalli site intensity can be specified. The local site conditions are described on two scales – geologic one, which samples the geology up to the depths of the order of kilometers, and local soil one, which samples soil properties near the surface up to depths of two hundred meters. The classification based on geology can be described by the categorical variable *geologic site condition* parameter $s$, which can take values 0 (sediments), 2 (rock), and 1 (intermediate site conditions), or by the depth of sediments $h$. The local soil classification is described by the categorical variable *local soil condition* parameter $s_L$, which can take on the values 0 ("rock" soil), 1 (stiff soil) and 2 (deep soil).

## 3. RESULTS

The methodology is illustrated for a scenario earthquake. A suite of synthetic motions and strains are presented for different earthquake sizes, hypocentral distances, and dispersion models, at a site and an array of sites. The target Fourier spectra were computed using the MMI-SITE-SOIL model (Trifunac

and Lee 1985). Synthetic motions were computed at 4096 points in time with time step 0.02 s, i.e. with total length of about 82 s. The trigger time was adjusted by shift of 5 s.

Figs 4 show snapshots of the radial, vertical and transverse synthetic accelerations at six sites, 100 m apart in the radial direction, with the closest site at $R = 10$ km distance from M6.5 earthquake. They were unfolded in time with dispersion model 3, and with $x = 4$ km. Noticeable differences in the acceleration time histories can be seen even though the sites are very close to each other. The differences, created by a purely deterministic physical model of wave propagation, are more complex than single phase shift and some small amplitude decay. The displacements, having more energy in the lower frequency part of the spectrum, differ much less at such small distances, because the lower frequency energy propagates with much larger velocities $U(\omega)$. They exhibit a high degree of similarity of the waveforms even at distances several kilometers away, as it can be seen in Fig. 5, which shows radial, vertical and transverse synthetic displacements at sites 1 km apart in the radial direction. Fig. 6 shows the agreement of the Fourier transform amplitudes of the synthetic motions and target spectra.

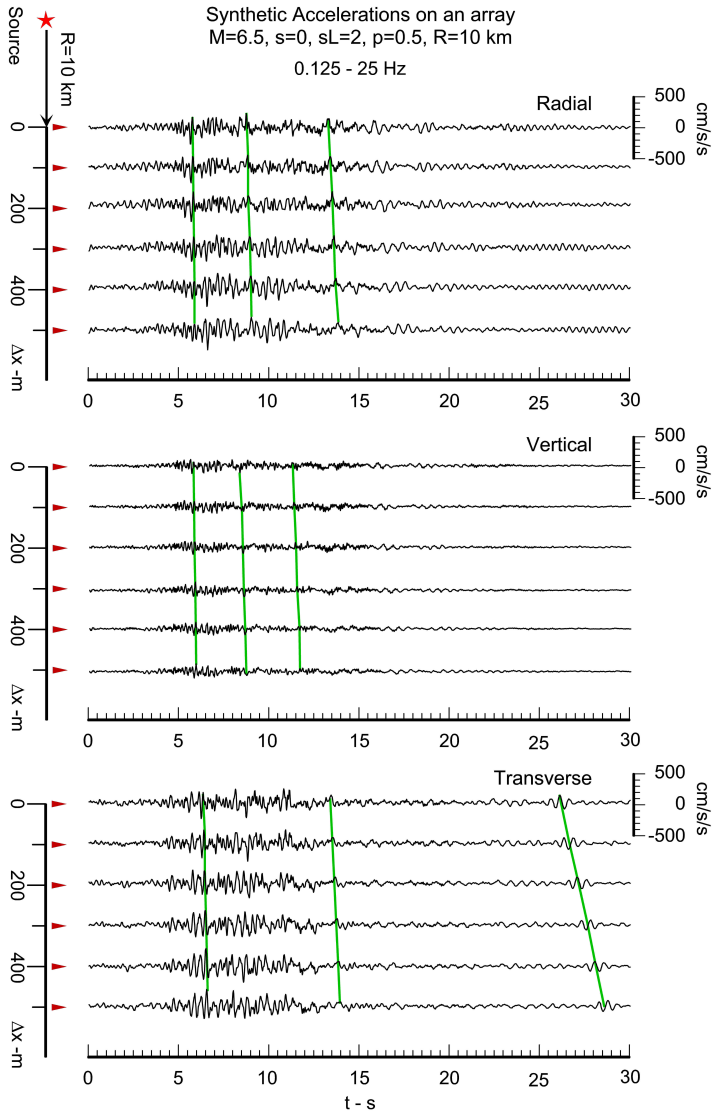


**Fig. 4** Snapshots of synthetic radial, vertical and transverse accelerations at 6 sites, 100 m apart in the radial direction, from M6.5 earthquake, at distance $R = 10$ km from the closest site, for site condition - sediments ( $s = 2$ ) and deep soil ( $s_L = 2$ ), unfolded with dispersion model 3.

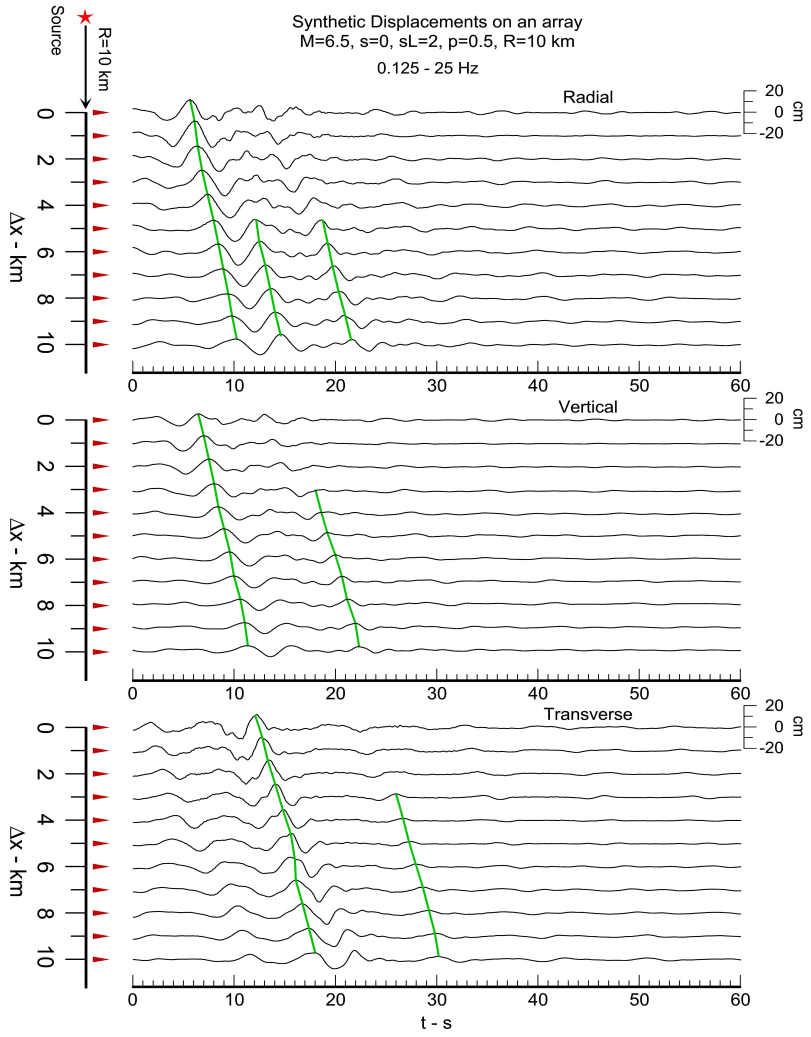


**Fig. 5** Same as Fig. 5 but showing synthetic displacements at 11 sites, 1 km apart.

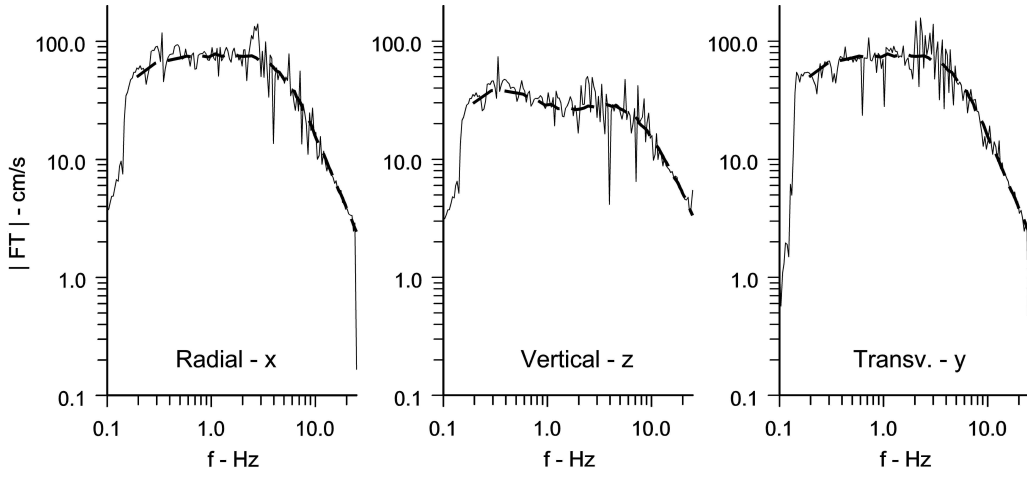


**Fig. 7** Fourier Transform amplitudes of synthetic accelerations in Figs 4, 5 and 6.

## 4. CONCLUSIONS

The updated SYNACC method for generation of multi-component synthetic time histories of earthquake ground motion at an array of points along the ground surface was presented, needed for design of long structures, pipelines and bridges, and in particular for nonlinear analyses in the time domain. The method combines empirical scaling laws for Fourier amplitude spectra of acceleration with a physical model of wave propagation in a horizontally layered half-space. Consequently, the amplitudes of the synthetic motions are consistent in statistical sense with observations, while the phase and local differences between points of the array are consistent with local characteristics of wave propagation. The presented examples showed that the method produces realistic and physically meaningful time histories.

## REFERENCES


Gabor D. (1946). Theory of communications, *J. of the Institute of Electrical Engineers - Part III: Radio and Communication Engineering*, **93**(26):429-457.

Gabor D. (1953). Communication theory and physics, *Institute of Radio Engineers, Professional Group on Information Theory,* **1**(1):48-59.

Haskell NA. (1953). The dispersion of surface waves in multilayered media, *Bull. Seism. Soc. Am.* **43**:17-34.

Lee VW (1990). Surface strains associated with strong earthquake shaking, *Proc. J.S.C.E., 422(n* I-14), 187-194.

Lee VW (2002). Empirical scaling of strong earthquake ground motion - Part III: Synthetic Strong Motion, *ISET J. of Earthquake Technology*, Paper No. 427, **39**(4):273-310.

Lee VW, Trifunac MD (1985a). Uniform risk spectra of strong earthquake ground motion. *Report No. 85-05*, Dept. of Civil Engrg., U. So. California, Los Angeles, California.

Lee VW, Trifunac MD (1985b). Torsional accelerograms, *Int. J. Soil Dyn. Earthq. Eng.*, **4**(3):132-139.

Lee VW, Trifunac MD (1987). Rocking strong earthquake accelerations, *Int. J. Soil Dyn. Earthq. Eng.*, **6**(2):75-89.

Mehta K, Snieder R, Graizer V. (2007). Extraction of near-surface properties for a lossy layered medium using the propagator matrix, *Geophys. J. Int.*;**169**:271-280.

Thompson WT. (1950). Transmission of elastic waves through a stratified solid, *J. of Applied Physics*, **21**:89-93.

Todorovska MI, Trifunac MD, Lee VW, Orbović N (2012). Synthetic earthquake ground motions on an array, *Soil Dyn. Earthq. Eng.*, submitted for publication.

Trifunac MD (1971). A method for synthesizing realistic strong ground motion, *Bull. Seism. Soc. Amer.*, **61**:1739-1753.

Trifunac, MD. (1976). Preliminary empirical model for scaling Fourier amplitude spectra of strong ground acceleration in terms of earthquake magnitude, source to station distance and recording site conditions, *Bull. Seism. Soc. Amer*., **66**:1343-1373.

Trifunac, MD. (1979). Preliminary empirical model for scaling Fourier amplitude spectra of strong motion acceleration in terms of Modified Mercalli Intensity and geologic site conditions, Earthqu. Engng Struct. Dynam., **7**:63-74.

Trifunac MD. (1989a). Dependence of Fourier spectrum amplitudes of recorded strong earthquake accelerations on magnitude, local soil conditions and on depth of sediments, *Earthq. Eng Struct. Dyn.*, **18**(7):999-1016.

Trifunac MD (1989b). Scaling of Fourier spectrum amplitudes of recorded strong earthquake accelerations in terms of magnitude and local soil and geologic conditions, *Earthq. Eng Eng Vib*., **9**(2):23-44.

Trifunac MD (1990). Curvograms of strong ground motion, *ASCE, EMD*, 116(6), 1426-1432.

Trifunac MD. (1994). Q and high frequency strong motion spectra, *Soil Dyn. Earthq. Eng.*, **13**(3):149-161.

Trifunac MD, Lee VW (1985). Preliminary empirical model for scaling Fourier amplitude spectra of strong ground acceleration in terms of earthquake magnitude, source to station distance, site intensity and recording site conditions, *Report CE 85-03*, Dept. of Civil Eng., U. So. California, Los Angeles, California.

Wong HL, Trifunac MD (1978). Synthesizing realistic strong motion accelerograms, *Report No. 78-07*, Dept. of Civil Engrg., U. of So. California, Los Angeles, California.

Wong HL, Trifunac MD (1979). Generation of artificial strong motion accelerograms, *Int. J. Earthquake Eng. Struct. Dynamics*, **7**:509-527.

Zerva A. (2009). Spatial variation of seismic ground motions: modeling and engineering applications. CRC Press, Taylor and Francis Group, Boca Raton, Florida.